JOURNAL OF MATERIALS SCIENCE 22 (1987) 1857–1863

Stress dependency on ultrasonic wave propagation velocity

Part 2 *Third order elastic constants of steels*

SENNOSUKE TAKAHASHI
National Research Institute for Metals, 2-3-12 Nakameguro, Meguro-ku, Tokyo 153, Japan
RYOHEI MOTEGI
Tokyo Keiki Co., Ltd, Minami-Kamata, Ohta-ku, Tokyo, Japan

The theory of wave propagation in a stressed solid was applied to the measurement of ultrasonic wave propagating velocity through tensile specimens of carbon steels containing 0.2 to 0.5% C, and Murnaghan's third order elastic constants of both Eulerian and Lagrangian formulation were obtained for those steels. They were ten times as large as the second order elastic constants, and values of the Eulerian constant n in them largely changed with composition of specimens. It was found that there was a simple relation between the Eulerian and Lagrangian third order elastic constants.

1. Introduction

The measurements of higher order elastic constants were made by Lazarus [1] and Hearmon [2] on the single crystals of KCl, NaCl, CuZn, copper and aluminium, Hughes and Kelly [3] on polystyrene, iron and pyrex glass, and many other workers [4–16] by use of ultrasonic waves. The measurement of residual stress has also been developed as an application research [17–19].

The theory of the change of ultrasonic wave velocities propagating in stressed solids which was dealt with using the Murnaghan's third order elastic constants (TOE constants) was reported in the previous paper [20].

In this paper, the measurement method of Murnaghan's TOE constants by a propagating ultrasonic pulse was proposed and results obtained for both Eulerian and Lagrangian TOE constants for four carbon steels containing 0.2 to 0.5% C and the relationship between the TOE constants by two formulae were described.

2. Measurement principle

The velocities of ultrasonic waves propagating in stressed isotropic materials can be expressed by the SOE and TOE constants [20]. On the basis of this theory, the authors determined the TOE constants by measuring the ultrasonic wave propagating velocities in unidirectional tensile stressed materials. In this case, high precision was needed for the geometrical form of the specimens, the measured values of stress, strain and ultrasonic wave velocities, and moreover the ambient temperature has also to be kept constant. The grip was the most troublesome part in the tensile stressed specimen. Since the waves of tensile direction passed through the complicated stress field of the grip section, the influence was unavoidable. In this experiment, two specimens which had identical grip length and cross-section of gauge region, but different gauge lengths, were prepared and the measurement data of wave velocities of the two specimens were used to eliminate the undesirable effect of the grip part.

2.1. An ultrasonic wave propagating along the tensile stress direction

The specimen shaped for tensile test, the coordinates, and the notation used in the formula are shown in Fig. 1. The ultrasonic wave sensor attached to the surface of the specimen end was used for measurement of the propagating time of the ultrasonic waves which enter from the left end and come back again by reflecting on the right end of the specimen.

Let V_{11} be the propagating velocity of longitudinal wave, and V_{12} be that of transverse one,

$$V_{11} = V_0\left(1 + \alpha_{11}\frac{\sigma_{11}}{E}\right)$$
$$V_{12} = V_0'\left(1 + \alpha_{12}\frac{\sigma_{11}}{E}\right) \quad (1)$$

where V_0 is the propagating velocity of longitudinal wave at non-stressed state, V_0' is that of the transverse wave, α_{11} is the relative change of longitudinal wave velocity, α_{12} is that of transverse wave, σ_{11} is the applied stress and E is the Young's modulus of the specimens. The first number of subscript of V indicates the propagating direction and the second one the polarization direction. The propagating time of longitudinal wave along tensile axis, t is given by

$$t = \frac{L_{G\sigma}}{\tilde{V}_{11G}} + \frac{L_Q}{V_0}\frac{(1 + \sigma_{11}/E)}{(1 + \alpha_{11}\sigma_{11}/E)} \quad (2)$$

Considering the grip and gauge region to be isolated, L_Q is the gauge length of the non-stressed specimen, L_G is the grip length of the non-stressed specimen, $L_{G\sigma}$ is that of the stressed specimen, and

0022–2461/87 $03.00 + .12

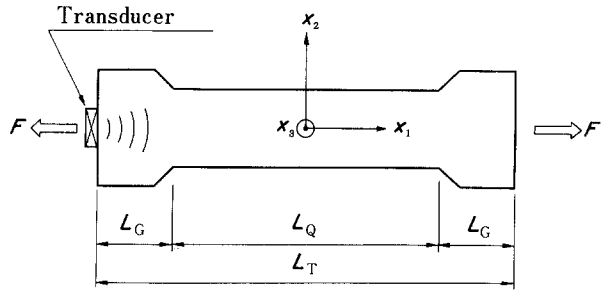

Figure 1 Specimen, coordinates, and notation used in the formula. x_1, x_2, x_3; coordinate axes, F; tensile force, L_G; grip length, L_Q; gauge length, L_T; total length of specimen.

$\tilde{V}_{11G}$ is the mean velocity of the longitudinal wave propagating through the grip region.

Since the stress at the grip region is very complicated, the first term of Equation 2 should be eliminated and two specimens which have identical grip size but different gauge length were prepared for this reason. The subscripts a and b are used to distinguish above two specimens. Letting t_{0a}, t_{0b} be the wave propagating time of non-stressed specimens a and b, and t_a, t_b be those of stressed ones, they are related by

$$t_{0a} = \frac{L_{Ta}}{V_0}, \qquad t_{0b} = \frac{L_{Tb}}{V_0}$$

and $\Delta t_a = t_a - t_{0a}$, $\Delta t_b = t_b - t_{0b}$ where L_{Ta} is the whole length of non-stressed specimen a, and L_{Tb} is that of non-stressed specimen b. L_{Qa} and L_{Qb} also mean the gauge length of non-stressed specimens a and b, respectively. The changing ratios of the propagating time are

$$\frac{\Delta t_a}{t_{0a}} = \frac{(L_{G\sigma}/\tilde{V}_{11G}) - (L_G/V_0)}{(L_{Ta}/V_0)} + \frac{L_{Qa}}{L_{Ta}}(1 - \alpha_{11})\frac{\sigma_{11}}{E}$$

$$\frac{\Delta t_b}{t_{0b}} = \frac{(L_{G\sigma}/\tilde{V}_{11G}) - (L_G/V_0)}{(L_{Tb}/V_0)} + \frac{L_{Qb}}{L_{Tb}}(1 - \alpha_{11})\frac{\sigma_{11}}{E} \qquad (3)$$

The term concerning the grip region can be eliminated from Equation 3.

Then

$$\alpha_{11} = 1 - \frac{E}{\sigma_{11}}\left[\frac{L_{Tb}}{\Delta L}\left(\frac{\Delta t_b}{t_{0b}}\right) - \frac{L_{Ta}}{\Delta L}\left(\frac{\Delta t_a}{t_{0a}}\right)\right] \qquad (4)$$

where $\Delta L = L_{Qb} - L_{Qa} = L_{Tb} - L_{Ta}$. In a similar manner, α_{12} can also be derived for the transverse waves from the changing ratio of the propagating time

$$\alpha_{12} = 1 - \frac{E}{\sigma_{11}}\left[\frac{L_{Tb}}{\Delta L}\left(\frac{\Delta t'_b}{t'_{0b}}\right) - \frac{L_{Ta}}{\Delta L}\left(\frac{\Delta t'_a}{t'_{0a}}\right)\right] \qquad (5)$$

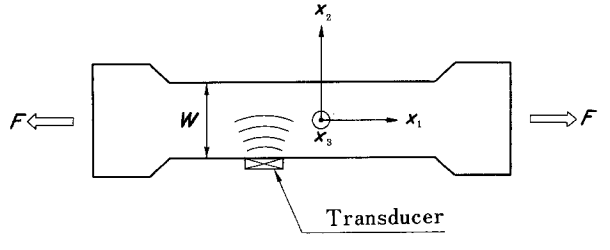

Figure 2 Tensile direction, wave propagating direction and coordinate. W; parallel part width.

where t' is the propagating time of the transverse wave.

2.2. An ultrasonic wave propagating along the direction perpendicular to tensile axis

Three kinds of wave propagating along the direction perpendicular to tensile axis were considered as

$$V_{22} = V_0\left(1 + \alpha_{22}\frac{\sigma_{11}}{E}\right)$$

$$V_{21} = V'_0\left(1 + \alpha_{21}\frac{\sigma_{11}}{E}\right)$$

$$V_{23} = V'_0\left(1 + \alpha_{23}\frac{\sigma_{11}}{E}\right) \qquad (6)$$

where V_{22} is the velocity of longitudinal wave propagating perpendicular to tensile axis, V_{21} is the velocity of transverse wave propagating along perpendicular, but polarizing parallel to the tensile axis, and V_{23} is the velocity of the transverse wave propagating along and polarizing perpendicular to tensile axis.

The propagating time of longitudinal wave, t is

$$t = \frac{w(1 - \nu\sigma_{11}/E)}{V_0(1 + \alpha_{22}\sigma_{11}/E)} \qquad (7)$$

where w is the width of gauge region of non-stressed specimen, and ν is Poisson's ratio.

Fig. 2 shows the tensile direction, wave propagating direction and coordinates. Using the changing ratio of the propagating time described in the previous section,

$$\alpha_{22} = -\nu - \frac{E}{\sigma_{11}}\left(\frac{\Delta t}{t_0}\right) \qquad (8)$$

and similarly for the transverse waves,

$$\alpha_{21} = -\nu - \frac{E}{\sigma_{11}}\left(\frac{\Delta t'}{t_0}\right)$$

$$\alpha_{23} = -\nu - \frac{E}{\sigma_{11}}\left(\frac{\Delta t''}{t''_0}\right) \qquad (8')$$

where t_0 is the propagating time of the longitudinal wave in the non-stressed state, t'_0 and t''_0 are those of transverse waves whose polarization are parallel and normal to tensile axis, respectively. $\Delta t/t_0$, $\Delta t'/t'_0$ and $\Delta t''/t''_0$ are the changing ratios of propagating time for each of the above waves.

2.3. The relative change of wave velocity and the third order elastic constant

The relative changes α_{11} and α_{22} are given by the Eulerian elastic constants (l, m, n) [20] as:

$$\alpha_{11} = -\frac{1}{2(\lambda + 2\mu)}[7\lambda + 14\mu - 6l - 2\nu(3\lambda - 6l - 2m)]$$

$$\alpha_{22} = -\frac{1}{2(\lambda + 2\mu)}[3\lambda - 6l - 2m - 2\nu(5\lambda + 7\mu - 6l - m)] \qquad (9)$$

From Equation 9

$$l = \left[\frac{7 + 2\alpha_{11}}{6(1 - 2\nu)}\right](\lambda + 2\mu) - \nu\left[\frac{(3\lambda - 2m)}{3(1 - 2\nu)}\right]$$

$$m = -\left(2 + \frac{\alpha_{11} - \alpha_{22}}{1 + \nu}\right)(\lambda + 2\mu) - 3\mu \quad (10)$$

Since the measurement of propagating time was easier and steadier for a longitudinal wave than for a transverse wave, l and m were obtained from the data of longitudinal waves and Equation 10. The transverse waves were used to determine n and in this case V_{12} and V_{21} showed steady values. The relative changes, α_{12} and α_{21} are given in the previous paper [20] as

$$\alpha_{12} = -\frac{1}{2\mu}\left[\lambda + 2\mu + \frac{m}{2} - \nu\left(2\lambda + 4\mu + m + \frac{n}{2}\right)\right]$$

$$\alpha_{21} = -\frac{1}{2\mu}\left[\lambda + 4\mu + \frac{m}{2} - \nu\left(2\lambda + 2\mu + m + \frac{n}{2}\right)\right] \quad (11)$$

Letting n_{12} be the value obtained from α_{12}, and n_{21} be the value from α_{21}, we have

$$n_{12} = \frac{2}{\nu}\left[(1 - 2\nu)\left(\lambda + 2\mu + \frac{m}{2}\right) + 2\mu\alpha_{12}\right]$$

$$n_{21} = \frac{2}{\nu}\left[(1 - 2\nu)\left(\lambda + \mu + \frac{m}{2}\right) + \mu(3 + 2\alpha_{21})\right] \quad (12)$$

n is only one for an isotropic solid, hence $n_{12} = n_{21}$.

2.4. Eulerian and Lagrangian TOE constants

α_{11}, α_{22}, α_{12} and α_{21} can be written with the Lagrangian TOE constants (l', m', n') from the equation of Hughes and Kelly [3] as

$$\alpha_{11} = \frac{1}{2(\lambda + 2\mu)}[5\lambda + 10\mu + 2l' + 4m' - 2\nu(\lambda + 2l')]$$

$$\alpha_{22} = \frac{1}{2(\lambda + 2\mu)}[\lambda + 2l' - \nu(6\lambda + 10\mu + 4l' + 4m')]$$

$$\alpha_{12} = \frac{1}{2\mu}\left[\lambda + 4\mu + m' - \nu\left(2\lambda + 2\mu + 2m' - \frac{n'}{2}\right)\right]$$

$$\alpha_{21} = \frac{1}{2\mu}\left[\lambda + 2\mu + m' - \nu\left(2\lambda + 4\mu + 2m' - \frac{n'}{2}\right)\right] \quad (13)$$

Since the values of α can be experimentally obtained, those of Equations 11 and 13 are identical.

Therefore the Lagrangian TOE constants are related to the Eulerian TOE constants as

$$l' = -2\lambda + 3l + m$$

$$m' = -2\lambda - 6\mu - \frac{m}{2}$$

$$n' = -12\mu + n \quad (14)$$

or

$$l = 2(\lambda + 2\mu) + \tfrac{1}{3}(l' + 2m')$$

$$m = -4\lambda - 12\mu - 2m'$$

$$n = +12\mu + n' \quad (15)$$

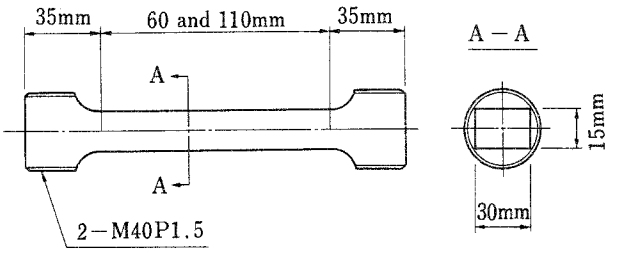

Figure 3 Dimension of test specimen.

3. Experimental details

3.1. Test specimen

The carbon steel samples were shaped for tensile test as shown in Fig. 3.

The precision of machining of the samples largely affects the measurement of wave velocity, therefore they were finished to within 2×10^{-6} m of planeness and within 5×10^{-6} m of parallelism. The size of test specimens was designed to be as large as possible to make the propagating path of the acoustic wave longer and to obtain precise measurements. The two types of specimen were prepared to eliminate the effect of grip region, which were identical in each dimension except the length of the gauge region. The four kinds of carbon steel, S20C(AISI 1020), S30C(AISI 1030), S40C(AISI 1039) and S50C(AISI 1049) were used for this experiment and their components were as shown in Table I. Each carbon steel of weight 50 kg were vacuum melted, cast into 25 kg ingots, forged, heat treated as shown in Table I, and shaped into specimens.

3.2. Sensor arrangement

The applied stress, strain and wave propagating time were strictly measured. Fig. 4 shows the arrangement of the strain gauges and ultrasonic wave transducers used for this experiment.

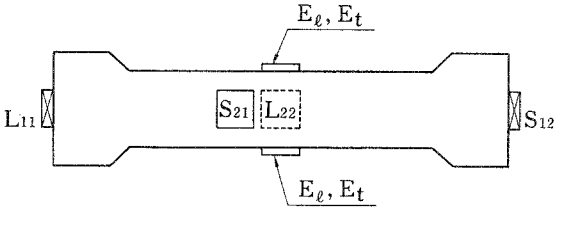

Figure 4 Arrangement of sensors. E_l, E_t; strain gauge, L_{11}, L_{22}; longitudinal wave transducer, S_{12}, S_{21}; transverse wave transducer.

TABLE I Chemical composition and heat treatment of test specimens

	Chemical composition (wt %)					Heat treatment
	C	Si	Mn	Ni + Cr	Cu	
S20C	0.22	0.29	0.52	–	0.01 max	880° C 3 h, air cooled
S30C	0.32	0.31	0.81	–	0.01 max	880° C 3 h, air cooled
S40C	0.40	0.28	0.78	0.12	0.01 max	860° C 3 h, air cooled
S50C	0.49	0.31	0.83	0.12	0.01 max	850° C 3 h, air cooled

Where F is the tensile direction, E_l and E_t are the strain gauges for measurement of strain parallel and normal to tensile direction respectively. They were attached by the adhesive of cyanoacrylate system. L_{11} and L_{22} are the transducers for ultrasonic longitudinal waves and S_{12} and S_{21} are those for transverse waves. The polarization of transverse waves transmitted and received by transducer S_{12} is normal but that by transducer S_{21} is parallel to the tensile axis. The piezoelectrical resonator of PZT type used as a transducer was a plate of $10 \times 10\,mm^2$ and the resonance frequency was 5 MHz.

3.3. Measurement method and apparatus

An Instron type tensile testing machine, a computerized strain measurement apparatus, ultrasonic wave propagating velocity measurement equipment were mainly used. The sing-around method [19] and the resonance frequency measurement method [21] need high technique to measure wave propagating velocity with good accuracy.

The method of superposing double pulses enables one to measure the wave propagating time directly, however the apparatus is very complicated [16]. Therefore in our experiment, it was measured by compensating the amplitudes of multi-echoes. Our apparatus and the operation were simple and easy to treat and gave high precision.

Fig. 5 shows a schematic diagram of this method. The pulser used was the type that discharged an accumulated electric charge and consisted of a cyristor as a switching element.

The -3dB bandwidth of the amplifier ranges were 0.5 to 8.0 MHz. The choice of echoes was carried out by using the degree of regularity of the propagating time of multi-reflection waves. Those times were measured using a comparator system. The counter consisted of 100 MHz quartz and gave good accuracy because of the time resolution of 10 nsec.

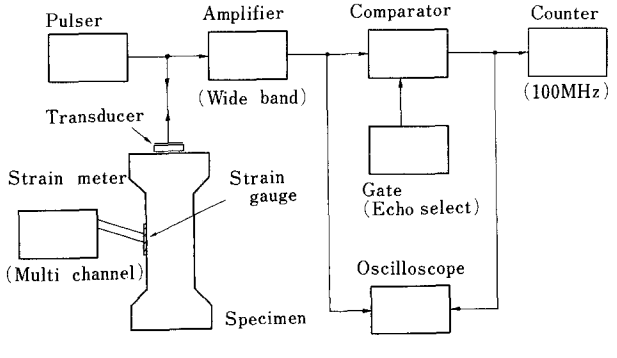

Figure 5 Measurement method and the schematic diagram.

The multi-echoes were compensated to make their level constant, and the time differences from the first echo to each echo was measured. The well regulated time differences were chosen among them in order to eliminate the influence of the sound field in the test specimen. Consequently, the reproducible data in the order of five figures was accomplished.

The cross-head speed of the tensile testing machine was held constant at $0.03\,mm\,min^{-1}$. The load cell used for measurement of stress was compensated by the standard gauge. The strain of the specimens was measured by the strain gauge adhered on the specimen surface and recorded by an auto multi digital recorder using an alternating current system. At that time, the obtained data were not affected by temperature since the room temperature was well controlled within 21 to 22° C throughout the measurement.

4. Results

4.1. Relative change of the propagating velocity

Fig. 6 shows the changing ratio of the propagating time of the longitudinal and transverse waves along the tensile axis for long and short size carbon steel specimens of S30C.

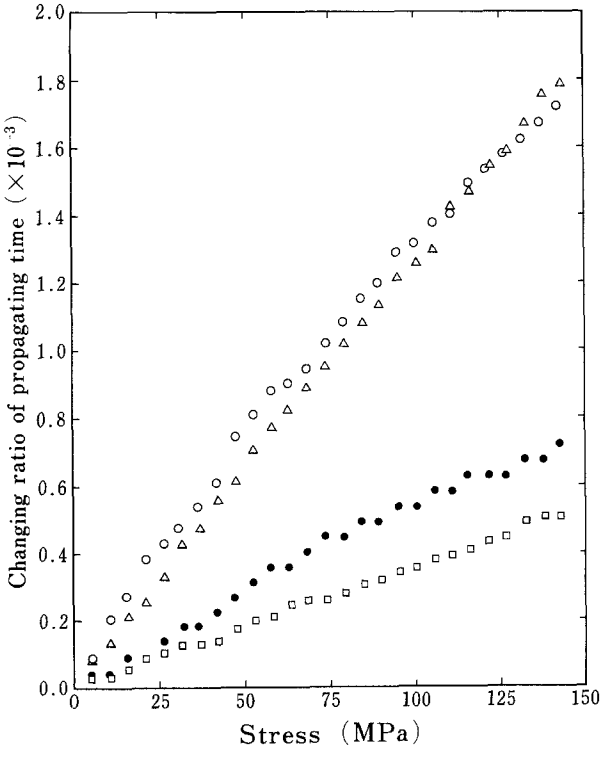

Figure 6 Changing ratio of propagating time of longitudinal and transverse waves along tensile axis for long and short specimens of S30C. Length of specimen (○) V_{11}, 130 mm, (△) V_{11}, 180 mm (□) V_{12} 130 mm and (●) V_{12} 180 mm.

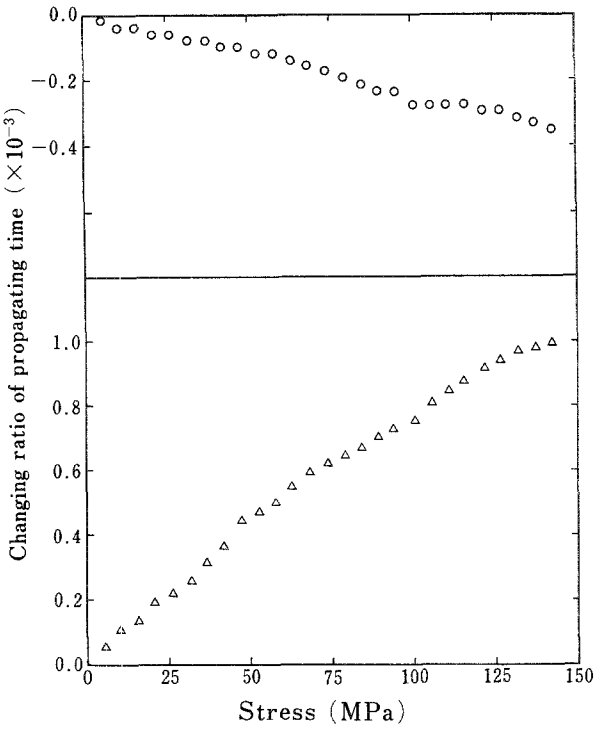

Figure 7 Changing ratio of propagating time when the wave propagates perpendicularly to tensile axis. (○) V_{22} (△) V_{21}.

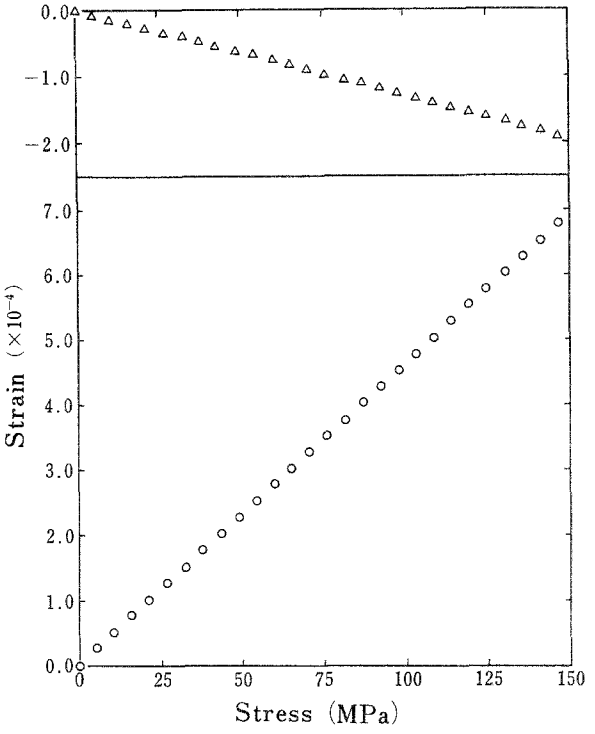

Figure 8 Stress–strain relation of S30C. (△) ε_t, (○) ε_l.

Fig. 7 shows the changing ratio of the propagating time when the ultrasonic wave propagates perpendicular to the tensile axis. The propagating time of the longitudinal wave decreased with tensile stress while that of transverse wave which was polarized to coincide with tensile direction increased. The measurement of the transverse wave whose polarization was normal to tensile direction could not be done on account of data irregularity. The similar results were obtained for S20C, S40C and S50C. Table II shows the relative change of propagating velocity obtained by substituting the above results into Equations 4, 5 and 8.

4.2. The second order elastic constant

Fig. 8 shows the stress–strain relationship of S30C. ε_l and ε_t denote the strain in the direction parallel and transverse to tensile axis, respectively. Stress is a nominal value which is the applied tensile load divided by cross-sectional area of gauge region of test specimen. Table IIIa shows the second order elastic constants (Lamé constants) λ and μ, obtained from above relations by using equations

$$\lambda = \frac{\nu E}{(1+\nu)(1-2\nu)}, \qquad \mu = \frac{E}{2(1+\nu)}$$

Table IIIb shows the SOE constants obtained by the measurement results of wave propagating velocities of longitudinal and transverse waves in the direction parallel and perpendicular to tensile axis of unloaded specimens. Table IV shows the above wave velocities.

4.3. The third order elastic constant

We can obtain the Eulerian TOE constants by putting the relative change of propagating velocity and SOE constants into Equations 10 and 12, and Lagrangian TOE constants by putting them into Equations 14.

Table 5 shows these results. The SOE and Eulerian TOE constants are plotted against carbon contents as shown in Fig. 9.

The TOE constants are about ten times the SOE constants and the values of n largely changed with carbon content of steels.

5. Considerations

Considering that the TOE constants systematically change with carbon content in a similar manner as the experimental results of ultrasonic wave propagating velocities [21], they were compared as shown in Fig. 9. As a result, it is recognized that the values of n in the TOE constants are dependent on carbon content except for the data of S20C. On the other hand the variations of SOE constants are about one order smaller than the values of n. Since the data were treated on the basis of the theory of isotropic materials in this experiment, the specimens were made

TABLE II Relative change of propagating velocity

	α_{11}	α_{22}	α_{12}	α_{21}
S20C	−1.856	0.528	−0.063	−1.374
S30C	−2.351	0.238	−0.844	−1.848
S40C	−2.004	0.177	−0.403	−1.497
S50C	−2.337	0.246	−0.220	−1.346

TABLE III The second order elastic constants ($\times 10^3$ MPa)

	(a) Isothermal elastic constants		(b) Adiabatic elastic constants	
	λ	μ	λ	μ
S20C	116.8	80.6	112.7	81.6
S30C	110.4	81.3	109.5	82.2
S40C	106.5	82.4	110.1	81.9
S50C	108.1	82.2	110.5	81.8

TABLE IV Measured velocities of longitudinal and transverse waves (m sec^{-1})

	V_{11}	V_{12}	V_{22}	V_{21}
S20C	5926	3225	5934	3225
S30C	5904	3229	5910	3242
S40C	5899	3223	5917	3239
S50C	5909	3223	5910	3234

as isotropic as possible. In order to confirm the isotropy of specimens, the wave propagating velocities were measured in the direction parallel and perpendicular to the longitudinal axis of the unloaded specimens. As is obvious from Table IV, the differences between them were negligible, so that the specimens could be regarded as isotropic for the SOE constants.

Furthermore the measurement values of n_{12} and n_{21}, or n'_{12} and n'_{21} were compared to ascertain the isotropy, and there were differences as shown in Table V. If the specimens are completely isotropic, n_{12} and n_{21} are equal, therefore they are considered as approximate isotropies.

In this method, an isothermal process is combined with an adiabatic process, namely, the static stress is applied to the specimen in the isothermal state and elastic waves propagate through it. According to the report by Krasil'nikov [22], the differences between isothermal and adiabatic TOE constants are small. Those differences of SOE constants were small and within experimental error in our experiments as shown in Table III, however a further problem is how the results from our method differ from the TOE constants measured in the adiabatic or isothermal condition only. This problem is related to the measurement method of TOE constants and the improvement of precision of the measurement.

The measurement precisions of our method are affected by those of stress, strain, propagating time and changing ratio, machining quality of specimens, atmospheric temperature control, etc. Among the above factors, the errors of about -0.9% in low load side and of about 0.3% in high load side were recognized for the load cell. The measurement precision of strain was in the range of 10^{-5} to 10^{-6} as read. Those of propagating time were stable and of the order of five figures. The changing ratio of propagating time were read from Figs 7 and 8, and the reading precision was ± 2 to $\pm 3\%$. The errors of changing ratio of propagating time and stress measurement largely affect l, m, n, of TOE constants and give maximum errors of 30, 10 and 50% on l, m and n, respectively.

Meanwhile the precision of data by Hughes and Kelly on armco iron was reported to be in the order of $\pm 100\%$ [3].

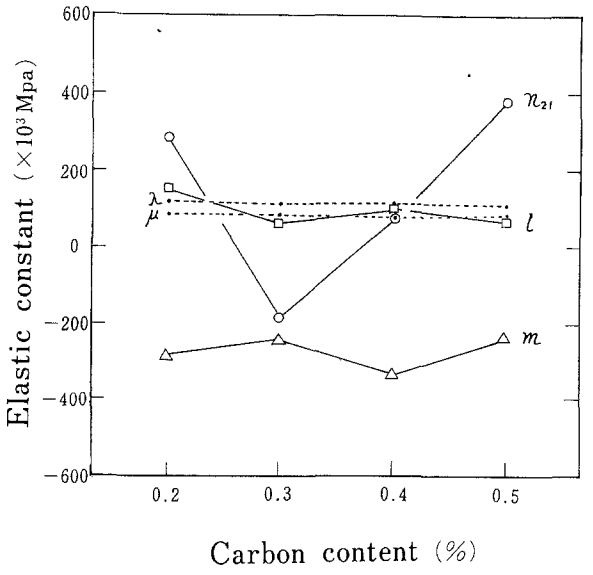

Figure 9 The SOE and Eulerian TOE constants against carbon content.

Wave propagating velocities of the increasing and decreasing processes of tensile load agreed well with each other as shown in Fig. 10. It is considered that the deformation was reversible and elastic during the test, therefore the change of wave propagating velocities corresponding to the elastic deformation were measured.

6. Conclusions

The theory of wave propagation in a stressed solid was applied to the measurement of the ultrasonic wave velocity propagating in tensile test specimens of carbon steels containing 0.2 to 0.5% C, and both Eulerian and Lagrangian TOE constants were obtained.

Two samples which were the same in grip size but different in gauge length were used in order to eliminate complex influences on ultrasonic wave velocity by stress distribution at the grip region. The TOE constants obtained were about 10 times as large as the SOE constants and the values of n showed large variation with the component of steels.

The Eulerian (l, m, n) and Lagrangian (l', m', n') TOE constants are written by simple relation including Lamé's constant are follows;

$$l = 2(\lambda + 2\mu) + \tfrac{1}{3}(l' + 2m')$$

$$m = -4\lambda - 12\mu - 2m'$$

$$n = 12\mu + n'$$

The values of n and n' give an index to determine the degree of isotropy of the materials.

TABLE V The Eulerian and Lagrangian third elastic constants ($\times 10^3$ MPa)

	Eulerian TOE constants				Lagrangian TOE constants			
	l	m	n_{21}	n_{12}	l'	m'	n'_{21}	n'_{12}
S20C	150.3	−286	287	304	−69	−574	−680	−663
S30C	62.5	−241	−183	−504	−274	−588	−1159	−1480
S40C	100.0	−328	80	−139	−241	−543	−909	−1128
S50C	67.0	−243	388	205	−258	−588	−598	−781

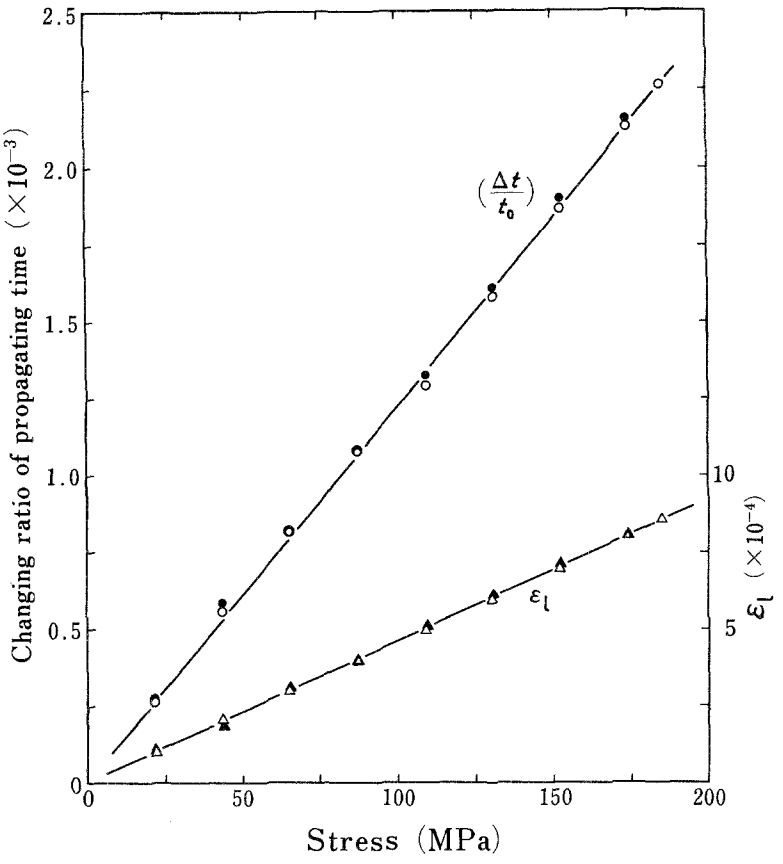

Figure 10 Hysteresis curves for the changing ratio and strain ε_l against tensile stress. The points were obtained from two measurements of increasing and decreasing stresses. (○, △) Increasing load, (●, ▲) decreasing load.

Acknowledgements

The authors would like to express their sincere appreciation to Dr Y. Higo who is the associate professor of Tokyo Institute of Technology, Research Laboratory of Precision Machinery and Electronics, for his advice in the experiments and to Mr Jun Tsuji, Tokyo Keiki Co., Ltd for his help in the preparation in the paper.

References

1. D. LAZARUS, *Phys. Rev.* **76** (1949) 545.
2. R. F. S. HEARMON, *Acta Crystallogr.* **6** (1953) 331.
3. D. S. HUGHES and J. L. KELLY, *Phys. Rev.* **92** (5) (1953) 1145.
4. H. J. McSKIMIN and P. ANDREATCH, *J. Appl. Phys.* **35** (1964) 2161.
5. A. L. STANFORD and S. P. ZEHNER, *Phys. Rev.* **136** (1967) A591.
6. Y. HIKI and A. V. GRANATO, *ibid.* **144** (1966) 411.
7. M. FISCHER, A. ZAREMBOWITCH and M. A. BREAZEALE, *Ultrason. Symp. Proc.* **2** (1980) 999.
8. J. E. MACKEY and R. T. ARNOLD, *J. Appl. Phys.* **40** (1969) 4806.
9. M. A. BREAZEALE and J. PHILIP, *J. Phys. (Orsay. Fr.)* **42** (C6) (1981) 134.
10. E. H. BOGARDUS, *J. Appl. Phys.* **36** (1965) 2504.
11. R. W. DUNHAM and H. B. HUNTINGTON, *Phys. Rev.* **B2** (1970) 1098.
12. W. T. YOST and M. A. BREAZEALE, *J. Appl. Phys.* **44** (1973) 1909.
13. G. K. WHITE and J. A. BIRCH, *Phys. Chem. Glasses* **6** (1965) 85.
14. F. R. ROLLINS, Jr, *International Advances in Non-destructive Testing* **5** (1977) 229.
15. D. E. EGLE and D. E. BRAY, *J. Acoust. Soc. Amer.* **60** (3) (1976) 741.
16. R. T. SMITH, R. STERN and R. W. B. STEPHENS, *ibid.* **40** (5) (1966) 1002.
17. D. I. CRECRAFT, *J. Sound Vib.* **5** (1) (1967) 173.
18. D. R. ALLEN and C. M. SAYERS, *Ultrasonic* July No. 4, **22** (1984) 179.
19. H. FUKUOKA and H. TODA, *Archives of Mechanics* **29** (5) (1977) 673.
20. S. TAKAHASHI and R. MOTEGI, *J. Mater. Sci.* **22** (1987) 1850.
21. S. TAKAHASHI, E. YAMAMOTO, N. UETAKE and R. MOTEGI, *ibid.* **13** (1978) 843.
22. O. M. KRASIL'NIKOV, *Sov. Phys. Solid State* **19** (5) May (1977) 764.

Received 14 July
and accepted 22 September 1986